# Regenerative Beam Extraction from the 150-Mev Synchrocyclotron at the Laboratoire Curie

N. F. Verster

Before describing this deflection work, I should like to say a few words about its historical background. Just over four years ago work started in Eindhoven on a 150-Mev proton synchrocyclotron for the Laboratoire Curie at Orsay near Paris. The method followed in the construction was as follows: The magnet was erected in Paris while the vacuum system, the r-f system, and the rest were built in Eindhoven. Afterwards, this equipment was moved to Orsay and the cyclotron was completely assembled. Consequently, the magnet was available in Paris for many months. We wanted to make the regenerative deflection system during this time when we had the magnet all to ourselves. On the other hand we had no beam to check the system. This called for a rather careful analysis. A small experimental computer, made at our laboratories, rendered excellent service in this analysis.

In my paper in Session IV, I described how the transition from stable oscillations to the deflection orbits can be studied by a smooth approximation. For the design of a deflection system this method is unsuitable and we have to study the successive orbits.

The method of calculating the coupled radial and axial oscillations during successive revolutions and for a sufficient number of initial conditions is laborious and not very instructive. If we disregard the influence of the axial amplitude on the radial orbits, however, the problem is much simpler. We determine the radial oscillations in the median plane and calculate then the axial oscillations of a particle following this radial orbit. We have determined the radial oscillations in the undisturbed cyclotron field from the sufficiently accurate equation,

$$r'' = r \frac{r_o B(r_o) - r B(r)}{r_o B(r_o)} \tag{1}$$

where B represents the magnetic induction in the median plane. The value of B and n (the field index) of our cyclotron is given in Figure 217.

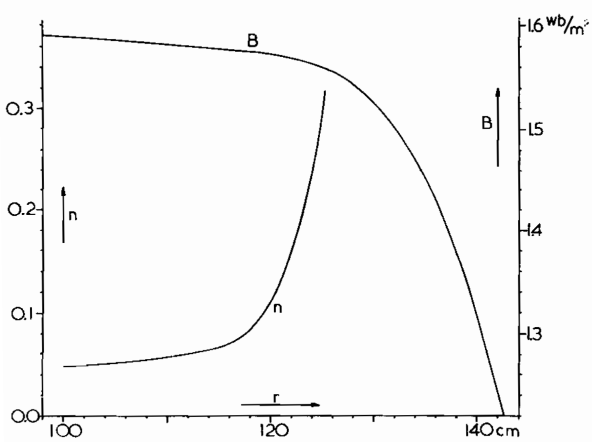


Fig. 217. The magnetic induction B(r) and the field index n(r) of the 150-Mev synchrocyclotron at the Laboratoire Curie.

The influence of the regenerator can easily be obtained if we make a thin lens approximation, i.e., if we define the regenerator strength I(r) by

$$I(r) = \int \frac{\Delta B}{B} r \, d\theta$$

where $\Delta B$ is the field distortion due to the regenerator. We assume that the center of the regenerator lies at $\theta = 0$. The influence on the orbits is given by

$$\Delta r = 0$$

$$\Delta r' = -(r/r_o)\, I(r)$$

We solve Eq. (1) for a number of amplitudes and introduce an azimuthal coordinate, $\psi$ (Fig. 218), fixed to the oscillation. The amplitude is characterized by $r_o'$ and the phase with respect to the regenerator by $\eta$, defined as

$$\eta = \psi - \theta.$$

We plot the calculated solutions of Eq. 1 in an $r - r_o$, $r'$ plane and obtain lines $r'_o$ constant and lines $\psi$ constant.

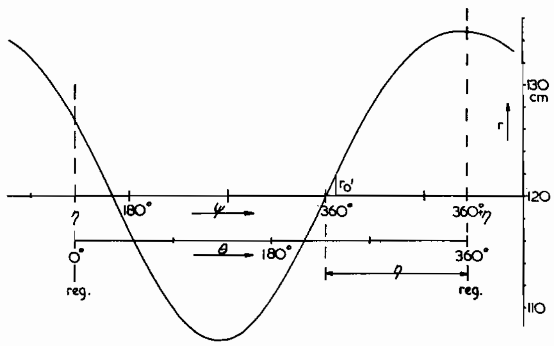


Fig. 218. A radial oscillation in the median plane. The amplitude is characterized by $r'_o$. The coordinate $\psi$ is fixed to the oscillation while $\eta$ gives the phase with respect to the regenerator.

The orbit of a particle during successive revolutions is now obtained in the following way (Fig. 219). During the interval $\theta = +0$ to $\theta = 2\pi - 0$ the particle moves along a line $r_o'$ constant from $\psi = \eta$ to $\psi = 2\pi + \eta$. In the regenerator the particle moves along a line $r$ = constant over a distance $\Delta r' = -(r/r_o)\, I(r)$. This gives us the value of $\eta$ and $r_o'$ of the next revolution and so on.

From this analysis we can obtain the following information.

(1) We can verify that the final phase does not depend much on the initial phase, as has been shown by Le Couteur[1] for the case of linear oscillations.

(2) We can determine a group of regenerator fields $I(r,\eta)$ which will give a constant phase angle $\eta$. These fields are a good starting point for determining the optimum regenerator (Fig. 220).

(3) For each regenerator field we can determine $r'_o$ and $\eta$ of the successive orbits, which will bring the particle into the channel.

(4) We find the separation of the successive orbits, the value of $r'$ at the entrance of the channel and also $dr'/dr$, i.e., the position of the virtual source of the beam entering the channel.

(5) We can estimate the influence of a local field error in the region $r > r_o$ by determining the corresponding value of $I(r)$, now located at a certain angle $\theta_e \neq 0$, and by estimating the influence of the corresponding shift in $r'$ at $\psi = \theta_e + \eta$ on the orbits.

The final choice of a regenerator field will not only be based on the amplitude and orbit separation obtainable at the channel entrance but also on the increase in axial amplitude at the entrance of the channel. The choice will depend on the kind of channel used.

---

[1] Le Couteur K. J. Proc. Phys. Soc. B (1951) 64, 1073.

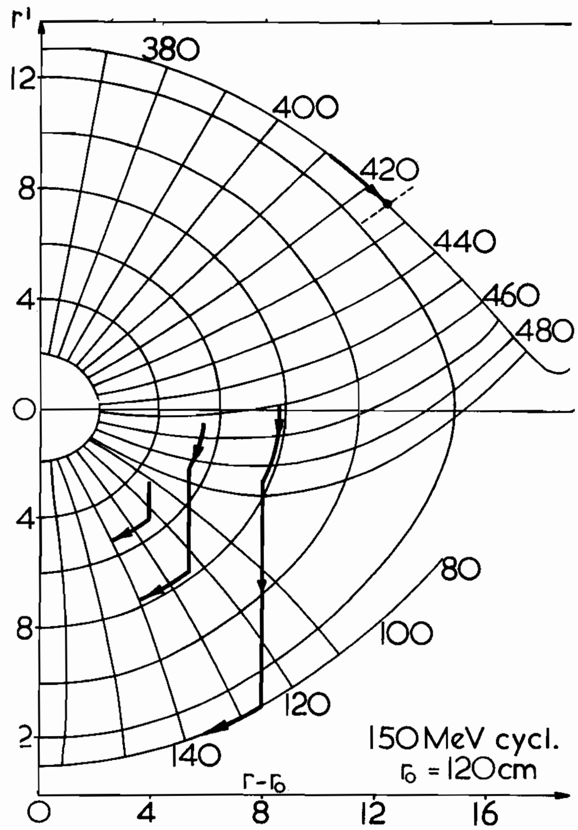


Fig. 219. Radial orbits of Fig. 218 are plotted in a $r - r_o$, $r'$ plane. A particle can graphically be followed through successive revolutions.

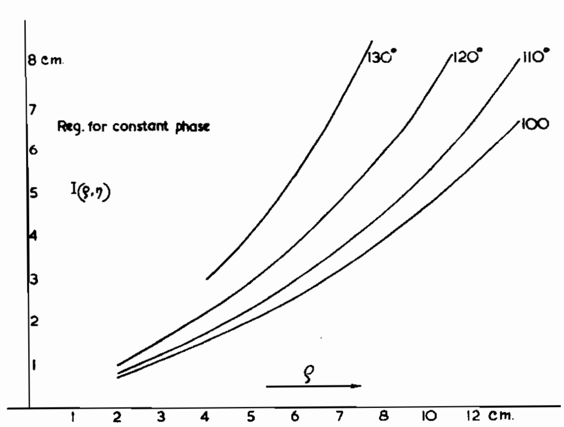


Fig. 220. Regenerator fields $I(r;\eta)$ for a constant phase $\eta$.

For determinating the increase in axial amplitude we used a method closely related to the method described by Le Couteur. The basis of this analysis is the calculation of the transfer matrix P, describing one revolution from $\theta = + 0$ to $\theta = 2\pi - 0$. The matrix elements are a function of the parameters $r'_o$ and $\eta$, characterizing the radial orbit $r(\theta)$. Figure 221 shows the calculated matrix elements. The influence of the regenerator is given by a transfer matrix

$$T = \begin{Vmatrix} 1 & 0 \\ \frac{1}{r_o}\frac{dI}{dr} & 1 \end{Vmatrix} .$$

From the analysis of both radial and axial oscillations we decided that a regenerator field $I(r) = 0.34\ (r - 120\ \text{cm}) + 0.07\ \text{cm}^{-1}\ (r - 120\ \text{cm})^2$ is suitable. The first coefficient gives an extraction radius of 120 cm, the second coefficient should lie between 0.06 and 0.08. We calculated this value under the assumption that the angular extent of the regenerator is zero. The appreciable length of our regenerator requires a correction, giving a second coefficient of about 0.08. The phase angle is $125^o \pm 1^o$ for the successive orbits.

Mr. van Mechelen was responsible for the entire cyclotron project; the deflection system was realized by Mr. de Kruiff and Mr. Smits. The regenerator field was produced quite accurately, while the remaining field errors due to imperfect shimming were well below the calculated limits. The channel was lined up along the orbit by the copper wire technique.

As is well known, the orbit of a flexible wire carrying a current i and under a tension T will be equal to the orbit of a particle of momentum p and charge e if $T/i = p/e$. The accurate calibration of T and i with respect to $r_o\ B(r_o) = p/e$ is difficult, however, and the reproducibility is limited by the friction in the pulley. Therefore,

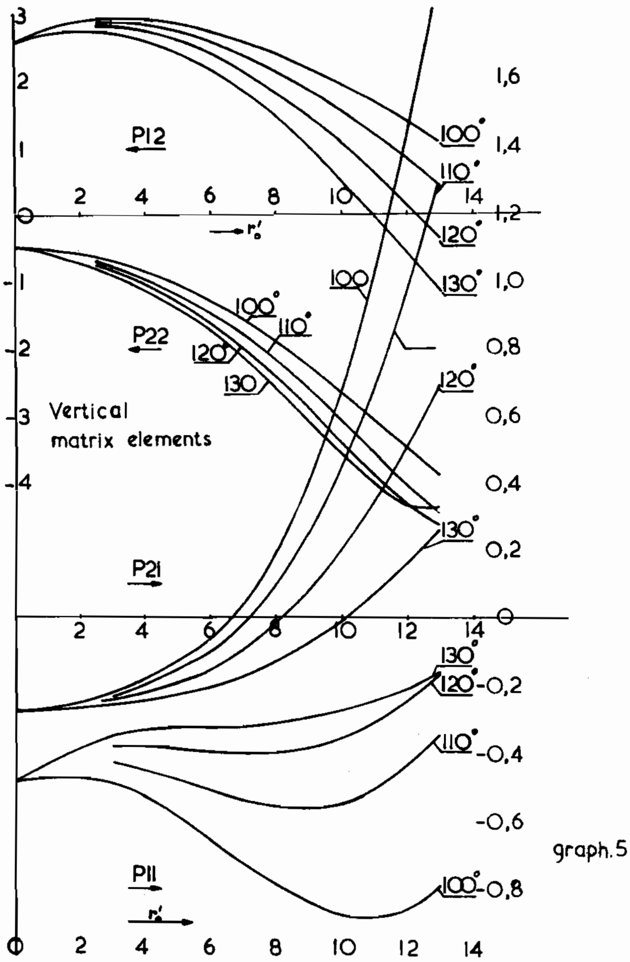


Fig. 221. Matrix elements of the vertical transfer matrix.

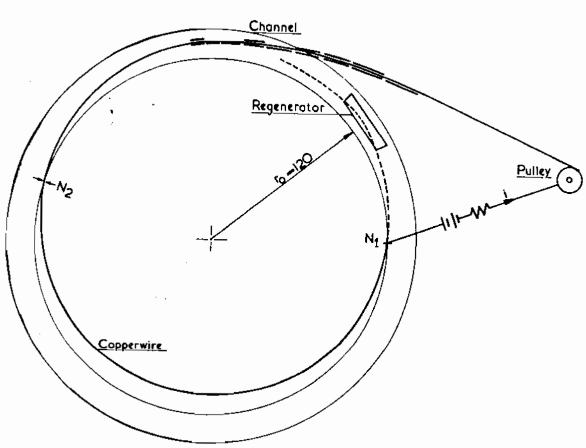


Fig. 222. Alignment of the channel with a copper wire. The wire is fastened at $N_1$ and the length is adjusted until the wire passes through $N_2$.

we used a method suggested by R. S. Livingston; we used the last half revolution as "180° spectrometer" for the wire (Fig. 222). The positions of the nodes $N_1$ and $N_2$ follow from the phase of the last oscillation and the calculated orbit. The wire is fixed at $N_1$. The length is then adjusted until the wire passes through $N_2$. The tension will adjust itself to the current. The orbit is reproducible to a millimetre or less.

The layout of the deflection system is shown in Figure 223. Figure 224 gives the regenerator with the main correction shims, and Figure 225 shows the deflection system in the cyclotron as seen from the port next to the ion source gate.

After the completion and testing of the cyclotron, the deflection system was tested with the beam. No adjustment of the regenerator or the channel was necessary. The deflection efficiency depends critically on the adjustment of the ion source conditions. An efficiency of 7% (6 μa internal, 0.4-0.5 μa external) was obtained regularly, an efficiency of 11% with 2 μa internal current was the maximum obtained. Finally, Figure 226 shows the beam after traveling 3 meters through air from the exit port. We have no measured data yet on the energy spread, but from the analysis described in my earlier paper we estimate an energy spread of a few tenths percent.

L. SMITH: How much work is involved in getting the proper field shape? Have you any opinion on the use of such devices on the variable-energy cyclotron?

VERSTER: The amount of work is considerable. We produced the field changes with almost or entirely saturated iron. This method is not suited for a variable-energy cyclotron. For a cloverleaf cyclotron the situation is moreover rather different as the radial

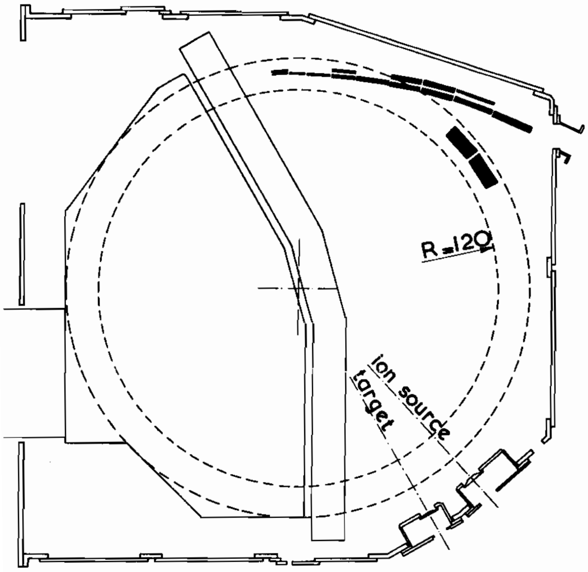


Fig. 223. Schematic layout of the deflection system.

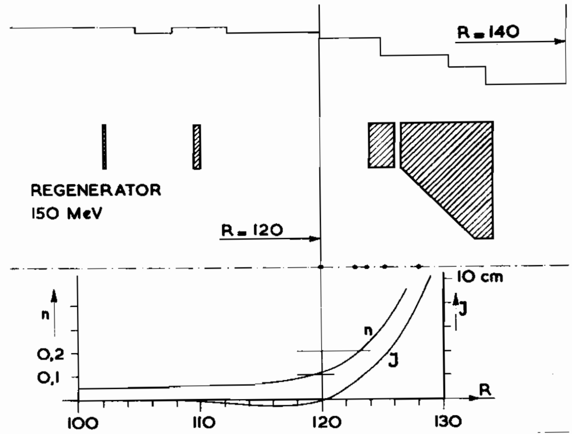


Fig. 224. Schematic cross-section of the regenerator with the main correction shims. The lower half gives the field index and the regenerator strength I(r). The dots represent respectively the position of the equilibrium orbit $r_o$ and the last deflected orbits.

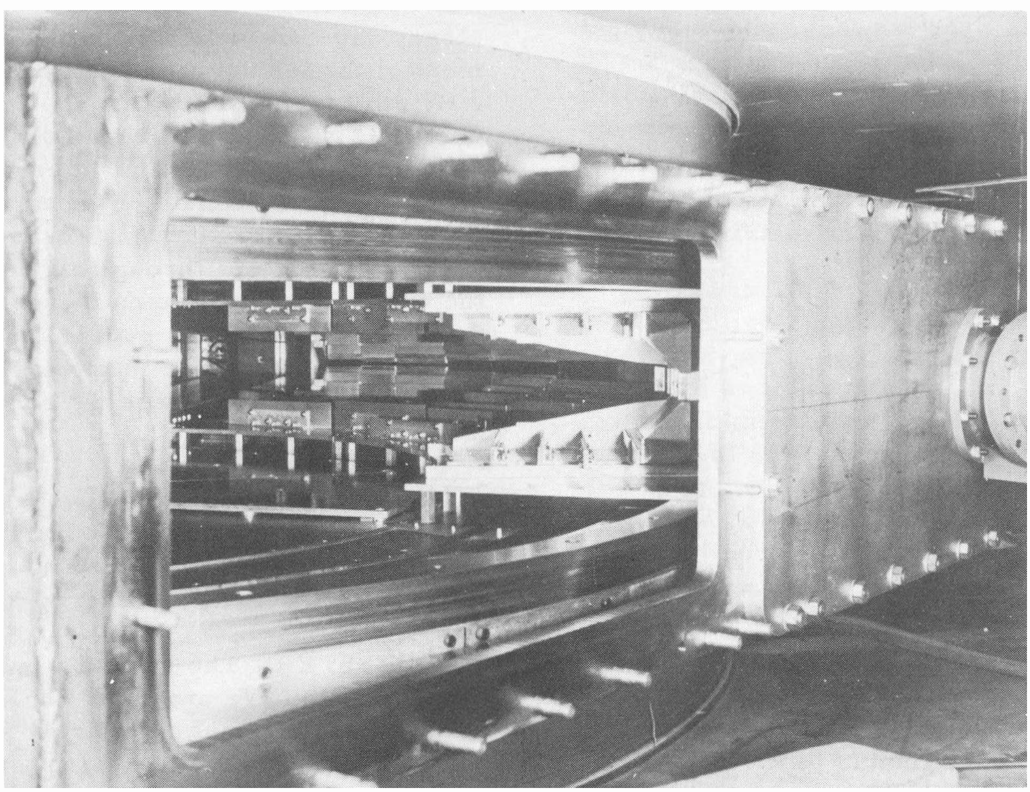

Fig. 225. The deflection system, seen from the port near the ion source gate. The entrance of the channel is in the background. The regenerator is clearly visible in the center. To the extreme right is the beam port.

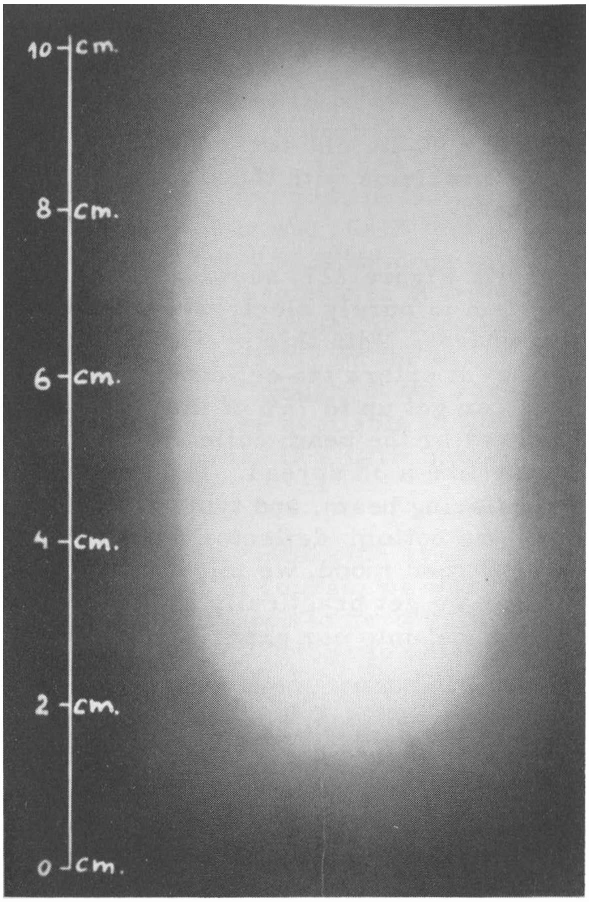


Fig. 226. Autoradiographic picture of the beam, three meters after the beam port (through air).

betatron frequency is higher than unity instead of lower, while the fundamental resonance, used in this deflection system, coincides with the 3/3 or 4/4 subresonance.

CHAIRMAN WELTON: Can you distinguish between efficiency of extraction into a channel and efficiency of ion transmission through the channel?

VERSTER: Practically all the beam is deflected. The orbit separation near the channel entrance is of the order of 4.5 cm, while the effective width of the channel entrance is 7 mm. This means that only about 15% of the beam will enter the channel. No further loss is expected. A similar reasoning holds for the axial size of the beam.